chemosensors

Article

A Bright Squeezed Light Source for Quantum Sensing

Wenhai Yang [1], Wenting Diao [1], Chunxiao Cai [1], Tao Wu [1], Ke Wu [1], Yu Li [1], Cong Li [1], Chongdi Duan [1], Hanyang Leng [2], Ning Zi [3] and Xukun Yin [4,5,*]

[1] China Academy of Space Technology (Xi'an), Xi'an 710000, China
[2] Qian Xuesen Laboratory of Space Technology, Beijing 100094, China
[3] Biobase Disinfection (Shandong) Co., Ltd., Zibo 255000, China
[4] School of Physics and Optoelectronic Engineering, Xidian University, Xi'an 710071, China
[5] State Key Laboratory of Applied Optics, Changchun Institute of Optics, Fine Mechanics and Physics, Chinese Academy of Sciences, Changchun 130033, China
* Correspondence: xkyin@xidian.edu.cn

Abstract: The use of optical sensing for in vivo applications is compelling, since it offers the advantages of non-invasiveness, non-ionizing radiation, and real-time monitoring. However, the signal-to-noise ratio (SNR) of the optical signal deteriorates dramatically as the biological tissue increases. Although increasing laser power can improve the SNR, intense lasers can severely disturb biological processes and viability. Quantum sensing with bright squeezed light can make the measurement sensitivity break through the quantum noise limit under weak laser conditions. A bright squeezed light source is demonstrated to avoid the deterioration of SNR and biological damage, which integrates an external cavity frequency-doubled laser, a semi-monolithic standing cavity with periodically poled titanyl phosphate (PPKTP), and a balanced homodyne detector (BHD) assembled on a dedicated breadboard. With the rational design of the mechanical elements, the optical layout, and the feedback control equipment, a maximum non-classical noise reduction of -10.7 ± 0.2 dB is observed. The average squeeze of -10 ± 0.2 dB in continuous operation for 60 min is demonstrated. Finally, the intracavity loss of degenerate optical parametric amplifier (DOPA) and the initial bright squeezed light can be calculated to be 0.0021 and -15.5 ± 0.2 dB, respectively. Through the above experimental and theoretical analysis, the direction of improving bright squeeze level is pointed out.

Keywords: quantum sensing; bright squeezed light; intracavity loss; escape efficiency

Citation: Yang, W.; Diao, W.; Cai, C.; Wu, T.; Wu, K.; Li, Y.; Li, C.; Duan, C.; Leng, H.; Zi, N.; et al. A Bright Squeezed Light Source for Quantum Sensing. *Chemosensors* **2023**, *11*, 18. https://doi.org/10.3390/chemosensors11010018

Academic Editor: Guo-Hui Pan

Received: 14 November 2022
Revised: 13 December 2022
Accepted: 23 December 2022
Published: 25 December 2022

1. Introduction

Bright squeezed light is the redistribution of the amplitude and phase of a coherent state of light, which exhibits reduced uncertainty below the shot noise limit (SNL) for amplitude or phase, or any linear combination thereof, and increased uncertainty in the conjugate observable. It has been 40 years since it has been confirmed that squeezed light can improve measurement sensitivity beyond classical limits [1]. Squeezed light is envisioned to have many practical applications, including optical sensing [2,3], quantum networks [4,5], quantum communication [6,7], quantum computation [8], and gravitational wave (GW) detection [9,10]. In particular, quantum sensing with squeezed light promises the ability to exceed classical performance limits [11]. The purported application domain for quantum enhanced sensors is vast: range-velocity and target-detection radars, squeezing−enhanced RF−photonic antennas, ultraprecise surface measurements with a non-classical probe, quantum enhanced gyroscopes, and entanglement-enhanced long−baseline telescopes just to name a few. In addition, there is an urgent need to improve the sensitivity of sensors in the biochemical and toxic gas detection fields [12–15]. All these applications require the long-term stability of the squeezed light source. Hence, a simple and reliable bright squeezed light source outside of the laboratory is needed. In this manuscript, we demonstrate a promising non-classical illumination source—the bright squeezed light source for quantum imaging and quantum sensing [16,17].

In order to develop a flexible and valuable squeezed light source, a variety of technologies were developed. From the early observation of squeezed state via four−wave mixing in atomic vapors [18] and parametric deamplification of quantum noise in optical fiber [19] to parametric down-conversion in the nonlinear crystal [20] and recent demonstrations of ponderomotive squeezing through optomechanical interactions [21–23], we can conclude that the most successful scheme for generating squeezed light is the parametric down-conversion. Indeed, the strongest vacuum squeezed light observed so far is −15 dB at the wavelength of 1064 nm [24]. The most advanced employment of a vacuum squeezed light source in GW observatories has achieved about 9 dB of squeezing up to 20 h, which uses a DOPA with a type−I PPKTP crystal. The non−classical light source is assembled on a 1.5 m^2 breadboard, which includes a full coherent control system and a diagnostic BHD [25]. However, the most simple and stable experiment device for a bright squeezed−light generation at 1064 nm was achieved by K. Schneider et al. [20].

Although tremendous progress in the experimental preparation of continuous-wave squeezed light has been achieved, the bright squeezed light source has not been used as a separate product for now. In order to achieve this goal, there are still some difficulties to overcome. For instance, long-term stability is a central issue, especially when the squeezed light is used as a useful tool for flexible applications. Therefore, it is necessary to develop a simple and reliable bright squeezed light source. In 2015, the group at Shanxi University experimentally demonstrated a compact entangled light source for practical applications in quantum information technology [26]. However, due to technical limitations, the long−term stability of the entangled light source is not good enough.

In this manuscript, a simple and long-term stable bright squeezed light source is developed as a real commercial product. To increase simplicity, a homemade single−frequency Nd: YVO_4/LBO laser with dual wavelength outputs is used [27]. Then, the second harmonic generation (SHG) and DOPA are constructed in a semi−monolithic standing cavity configuration. Meanwhile, the Pound–Drever–Hall (PDH) technique is adopted to lock both the cavity length at the resonance point of DOPA and the relative phase of π between the pump beam and the seed beam [28]. Then, the DOPA emits bright amplitude squeezed light, which can be detected with a BHD when the flip mirror is removed. A maximum non-classical noise reduction of -10.7 ± 0.2 dB is observed directly. The stable non-classical noise suppression of about -10 ± 0.2 dB is obtained over an hour. The practical advantages of simplicity and long-term stability make the developed bright squeezed light source suitable as a real commercial product for sub-shot-noise quantum sensing.

2. Experimental Setup

A schematic diagram of the setup for the squeezed light source is shown in Figure 1, which comprises four modules: a homemade single-frequency laser, a homemade DOPA, a homemade SHG, and a homemade control system. For clarity, some optical components are omitted. We try our best to achieve the shortest optical path from the homemade single−frequency laser to every optical resonator and with the least optical components needed to realize the optimal mode-matching between the laser beam and every optical resonator. After these steps are implemented, the configuration of the bright squeezed light source is minimized, the influence of the external environment interference on the source is weakened, and the system's mechanical stability is improved. All the optical components screw onto a custom cast aluminum base plate, which is strengthened by a rear grid frame. The dimension of the bright squeezed light source is about $750 \times 560 \times 180$ mm^3.

The DOPA and SHG are set up as a standing−wave of semi-monolithic cavity, containing a PPKTP crystal and an output-coupling mirror. The front surface of the PPKTP crystal is high-reflectivity coated at 1064 nm and anti−reflectivity coated at 532 nm for DOPA, while high-reflectivity coated at 1064 nm and 532 nm for SHG. The rear surface of the crystal is anti-reflection coated for both wavelengths in DOPA and SHG, respectively. The output-coupling mirror of the semi-monolithic standing-wave cavity is a piezo−actuated external mirror with high reflectivity at 532 nm and transmissivity of 12% at 1064 nm for DOPA,

and anti-reflectivity at 532 nm and transmissivity of 12% at 1064 nm for SHG, respectively. In addition, the front surfaces of PPKTP crystals are convex with a curvature of 12 mm, and the rear surfaces of the PPKTP crystals are flat, with a size of about $1 \times 2 \times 10$ mm^3. Since the curvature radius is 30 mm, the output−coupling mirror is placed on the rear surface of the PPKTP crystal at a distance of approximately 25 mm. Thus, the line width of DOPA and SHG can be calculated as 70.7 MHz. The DOPA is singly resonant at 1064 nm with the pump laser dual passing the PPKTP crystal. In addition, the temperature of the PPKTP crystal is stabilized to the phase-matching of the fundamental seed beam and the second harmonic pump beam. Figure 2 shows the internal structure of the quasi-monolithic DOPA, which can accommodate the copper oven of nonlinear crystal, Peltier and piezo−actuated output-coupling mirrors. The cavity is mechanically stabilized by concatenating mounts of the mirrors and the copper oven with a massive invar base.

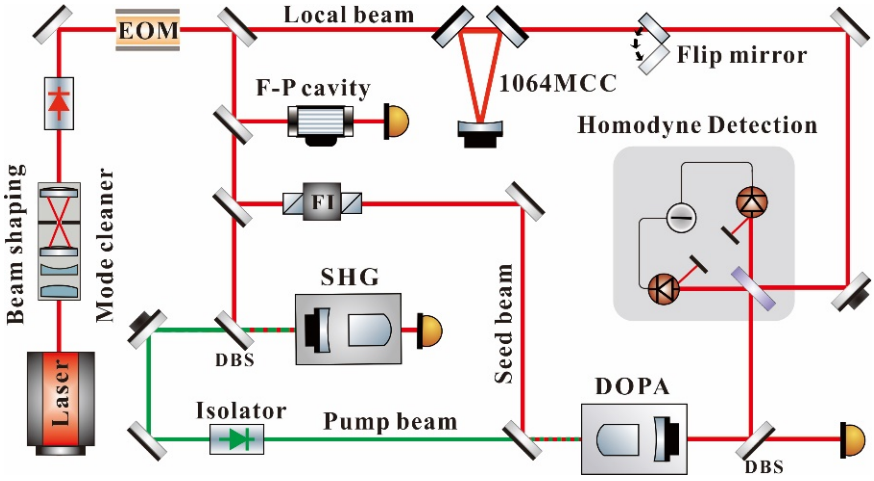

Figure 1. Schematic of the complete optical setup of the squeezed light source (SHG, second harmonic generation; EOM, electro-optic modulator; DBS, dichroic beam splitter; DOPA, degenerate optical parametric amplifier; MCC, mode cleaner cavity; F-P cavity, Fabry–Pérot cavity; FI, Faraday isolators).

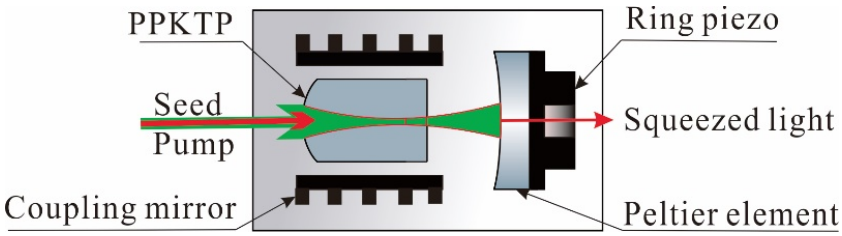

Figure 2. Internal structure of the quasi-monolithic DOPA.

The DOPA is driven by a homemade low-noise intracavity single−frequency Nd: YVO_4/LBO laser with dual wavelength outputs. The power at 532 nm and 1064 nm is about 380 mW and 15 W, respectively. The volume of this laser is about $200 \times 100 \times 80$ mm^3, and the M^2 value of the output beam is about 1.2. The power stability of the output laser at 1064 nm is shown in Figure 3. As shown in the illustration, the peak−to−peak fluctuation is better than ±1.3% for 8 h. The 1064 nm laser is divided into four parts after passing through a mode cleaner device to optimize the distribution of spatial mode and an electro-optical phase modulator to modulate the phase of the light field. A tiny fraction is injected into an F−P cavity to monitor the single frequency operation, as shown in Figure 4. The other three parts are injected into DOPA, the SHG cavity, and the mode cleaner cavity (MCC), which are used as the seed beam of DOPA, the fundamental frequency pump beam of the SHG, and the local oscillator (LO) for homodyne detection, respectively. Then, the 532 nm laser output from SHG is injected into DOPA from the front surface of the PPKTP crystal as the pump beam.

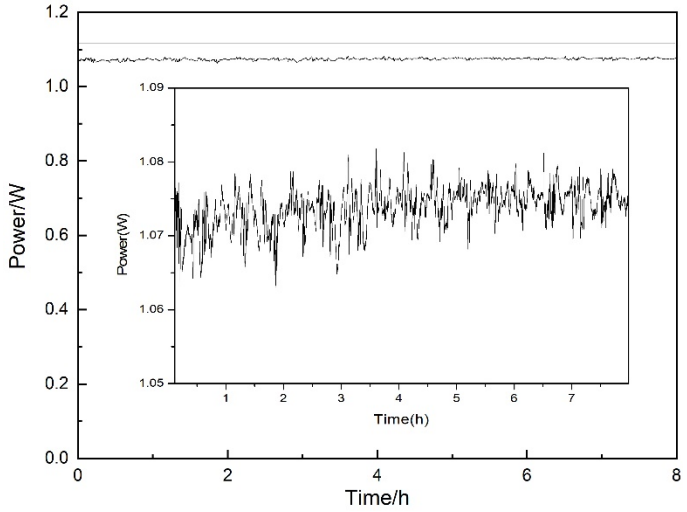

Figure 3. Power stability of the output laser at 1064 nm.

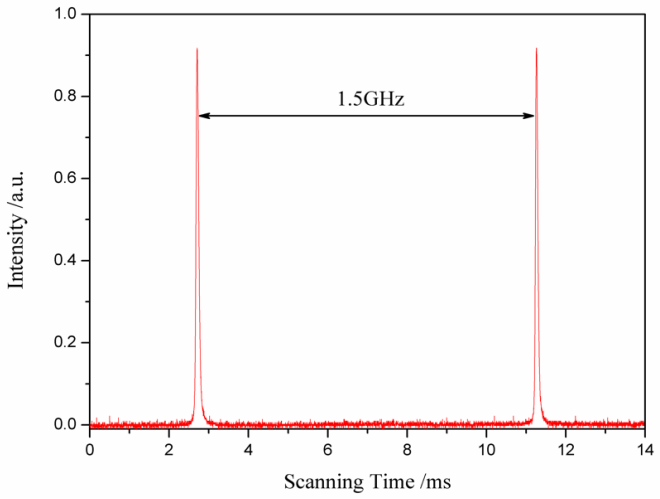

Figure 4. Single frequency operation of the output laser at 1064 nm.

The preparation and purpose of the seed beam and pump beam should be discussed in more detail. The seed beam through the Faraday rotation isolator (FI) and the half−wave plate is mode-matched and injected into DOPA with vertical polarization. Subsequently, the cavity length and π phase between the pump beam and the seed beam are stabilized using the seed beam transmitted through the DOPA, which is detected on the photodiode $PD_{OPA/\pi\text{-phase}}$. As a result, the error signal of DOPA's cavity length and the relative phase of the pump beam and the seed beam can be fed back onto the piezo−actuated output−coupling mirror of DOPA and the piezo−actuated steering mirror in the pump beam path, respectively. Both the DOPA's cavity length and the relative phase between the pump beam and the seed beam are locked, utilizing the PDH technique at an rf−modulation frequency of 35.6 MHz. With a redesigned high−gain resonance−type photo−detector to receive the transmitted light from DOPA, a seed beam with 5 mW is employed to implement the stable cavity length and π phase between the pump beam and the seed beam locking. In addition, the PDH technique is improved by adjusting the phase of another 35.6 MHz rf-signal, which is injected into the mixer to yield the error signal of π phase between the pump beam and the seed beam locking. The improved PDH technique realizes the theoretical control bandwidth of 71.2 MHz, which is conducive to achieving long−term stability of the bright squeezed light source.

The generated squeezed light is combined with the LO by employing a 50/50 beam splitter to generate an interference signal and detected by a homemade BHD with the

maximum common mode rejection ratio (CMRR) and clearance of 75.2 dB and 37 dB, which installed two arbitrary large−area InGaAs photodiodes (ETX500) of the same model [29]. The circuit noise level of the BHD at 3.7 MHz is nearly 25 dB below the shot noise level with the LO power of 12 mW, with the output of the BHD measured at the Fourier frequency of 3.7 MHz. In order to improve the homodyne efficiency, the LO is spatially filtered by the MCC, which yields the ideal Gaussian beam in fundamental mode. Then, the LO is transformed through a set of optical lenses to achieve the same spatial mode as the spatial mode of bright squeezed light output from DOPA. The relative phase between bright squeezed light and LO is locked by the improved PDH technique, which consists of a newly developed resonant electro−optic modulator and resonant photodetector [30,31], and the theoretical control bandwidth of the feedback loop reaches 71.2 MHz. As a result, it is conducive to reduce the phase jitter caused by environmental interference.

3. Experimental Results

The non−classical noise level of the bright squeezed light of DOPA output obtained by direct measurement is shown in Figure 5, which is observed when the pump power is 145 mW and the seed power is 5 mW. The -10.7 ± 0.2 dB squeezing and $+19.3 \pm 0.2$ dB anti-squeezing are successfully obtained by a spectrum analyzer (R&S FSW SIGNAL & SPECTRUM ANALYZER, 2 Hz, 26 GHz) in zero-span mode. The resolution bandwidth (RBW) and video bandwidth (VBW) are set to 300 kHz and 200 Hz, respectively. The non-classical noise average reduction of -10 ± 0.2 dB is detected directly in continuous operation over 60 min.

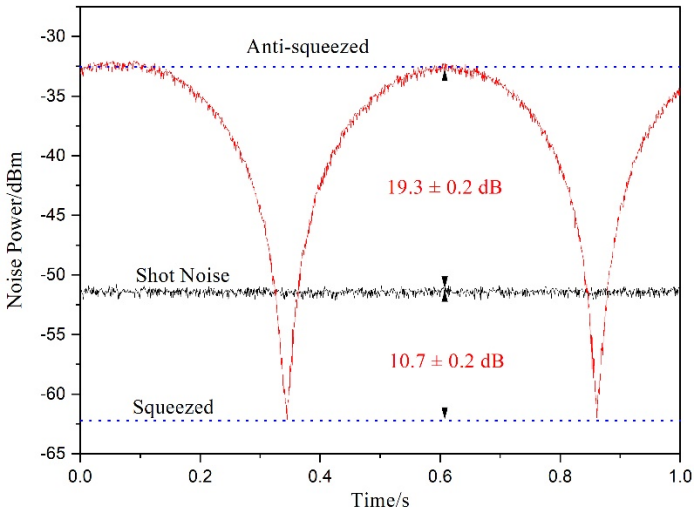

Figure 5. Noise power of squeezed light. Fourier frequency = 3.7 MHz, RBW = 300 kHz, VBW = 200 Hz.

4. Discussion

Theoretically, the non-classical noise power can be further squeezed significantly by increasing the power of the pump beam. However, higher pump power will bring a lot of problems. For example, the thermally−induced birefringence effect will lead to the deterioration of the light spot, which is caused by the absorption of the pump laser inside the PPKTP crystal. As a result, the locking stability and parameter down−conversion efficiency of DOPA will deteriorate simultaneously. In addition, the increase in pump power will lead to greater intracavity loss, which will lead to a decrease in the escape efficiency of DOPA. The following is a theoretical analysis of various factors affecting the non−classical noise level of the bright squeezed light.

The spectra of non-classical noise variances of the bright squeezed light output from DOPA can be expressed as

$$V_{a/s} = 1 \pm \frac{4(1 - l_{tot})\sqrt{P_{sh}/P_{th}}}{\left(1 \mp \sqrt{P_{sh}/P_{th}}\right)^2 + 4(f/\kappa)^2} \quad (1)$$

In the equation, P_{sh} is the pump power, P_{th} is the threshold value of DOPA, f is the Fourier frequency, κ is the line width of DOPA, and l_{tot} is the overall optical loss. The overall efficiency $\eta = 1 - l_{\mathrm{tot}} = \eta_{esc}\eta_{prop}\eta_{homo}\eta_{qe}$; where, η_{esc} is the escape efficiency of DOPA, which is the ratio of the output coupling decay rate to the total cavity decay rate, η_{prop} is the propagation efficiency of the bright squeezed light, which is related to the coating quality and absorption of the optical components, η_{homo} is the homodyne efficiency, which is the fringe visibility squared between the bright squeezed light and the LO light, and η_{qe} is the quantum efficiency of the photo diodes.

The propagation efficiency can be obtained according to the factory parameters of the optical component behind DOPA, which is about $\eta_{prop} = 0.995$. The homodyne efficiency is the fringe visibility squared between the bright squeezed light and the LO light, which can be expressed as

$$\eta_{homo} = VIS^2 = (I_{max} - I_{min})^2/(I_{max} + I_{min})^2 \quad (2)$$

where the maximum and minimum intensities I_{max} and I_{min} are measured with a high−gain DC detector in one of the output ports of 50/50 beam splitters by sweeping the relative phase between the LO light and the signal light. The signal light is the seed beam transmitted from DOPA and has the same power as the LO light. The experimentally−measured fringe visibility is $VIS = 0.998$, and the corresponding homodyne efficiency is $\eta_{homo} = 0.996$. The quantum efficiency can be obtained according to the factory parameter of a photo diode, which is $\eta_{qe} = 95\%$ (FD500 without AR−coated flat window cap). Thus, the product of $\eta_{prop}\eta_{homo}\eta_{qe} = 0.941$. Through experimental measurement, the threshold of DOPA can be obtained as $P_{th} = 206$ mW. Then, by substituting the relevant parameters into Equation (1), the overall efficiency and the escape efficiency can be respectively obtained as follows: $\eta = \eta_{esc}\eta_{prop}\eta_{homo}\eta_{qe} = 0.925$, $\eta_{esc} = 0.983$.

Then, the intracavity loss of DOPA and the non−classical noise reduction of the initial bright squeezed light can be derived based on the escape efficiency. The DOPA's escape efficiency is the ratio of the output coupling decay rate to the total cavity decay rate, and its expression is as follows

$$\eta_{esc} = T/(T + L) \quad (3)$$

In the equation, T is the power transmissivity of DOPA's output−coupling mirror and L is the intracavity loss of DOPA. According to the power transmissivity of the output−coupling mirror given in the previous section, the intracavity loss can be deduced to be $L = 0.0021$. Among all optical losses, only the intracavity loss of DOPA affects the non−classical noise reduction of the initial bright squeezed light output from DOPA, so the non−classical noise reduction of the initial bright squeezed light can be derived according to the escape efficiency, which is determined by the intracavity loss. Then, the non−classical noise reduction of initial bright squeezed light can be calculated by substituting the escape efficiency $\eta_{esc} = 0.983$ into Equation (1), which corresponds to -15.5 ± 0.2 dB of initial bright squeezed light. Since the propagation loss, homodyne detection loss and quantum loss of the photo diodes can be subtracted, and more than -15.5 ± 0.2 dB bright squeezed light will be directly injected into the quantum sensing system with squeezed enhancements technique in vivo applications (sub−shot−noise measurement system).

In addition, the stable output of bright squeezed light from DOPA depends on the stable pump power, the precision-controlled locking loop, the strong mechanical structure, and so on. Especially, the pump power stability of 532 nm is very important. The DOPA's cavity length is locked using the s−polarized seed laser, while the pump power fluctuations will change the thermal load, leading to the variation of crystal temperature. Thus, degradation of the phase−matching condition in PPKTP leads to the deterioration of the non−classical noise power of bright squeezed light. Meanwhile, the power dependence of the parametrical down-conversion efficiency may result in an even greater non−classical

noise power fluctuation of bright squeezed light, so the power stability of the pump beam is an important premise for the bright squeezed light generation. Through a specially designed low−noise external cavity, the frequency−doubled laser reaches the peak−to−peak of power fluctuation less than ± 1.3% for 8 h. With the optimization of the locking loop and power stable system, continuous locking over 60 min is achieved. Based on the organic combination of the above subsystems, the bright squeezed light source with continuous output over an hour is realized.

5. Conclusions

A simple and long-term stable bright squeezed light source is demonstrated as a commercial product, where the non-classical noise squeeze of −10.7 ± 0.2 dB and anti−squeeze of +19.3 ± 0.2 dB are directly observed and the non−classical noise average reduction of −10 ± 0.2 dB is demonstrated over the entire 60 min. Therefore, the squeezed light source has to be ready to implement quantum sensing for in vivo application (sub−shot−noise measurement system). In addition, the escape efficiency of the DOPA cavity can be deduced based on the relevant system parameters and experimental data. The relevant system parameters include propagation efficiency, homodyne efficiency, and quantum efficiency. The relevant experimental data include the squeezed non-classical noise power, and the DOPA's pump power and threshold. Then, the intracavity loss of DOPA and the non−classical noise reduction of the initial bright squeezed light output from DOPA can be deduced by taking the escape efficiency into account. Finally, the intracavity loss of DOPA and the non−classical noise reduction of the initial bright squeezed light can be calculated to be 0.0021 and −15.5 ± 0.2 dB, respectively. Through detailed analysis and description of the negative factors affecting the non−classical noise squeezed, it lays a foundation for improving the squeeze level. Next, we plan to develop a better−performing electro−optic modulator and a high−gain detector for cavity length locking and relative phase locking of two optical fields, which will provide a more stable feedback control technique for the further development of squeezed light source.

Author Contributions: Conceptualization, W.Y. and X.Y.; methodology, W.Y.; software, W.D. and C.C.; validation, W.Y., Y.L., C.L., T.W., K.W., H.L. and N.Z.; formal analysis, X.Y.; investigation, W.Y. and X.Y.; resources, W.Y. and C.D.; data curation, W.Y. and X.Y.; writing—original draft preparation, W.Y. and X.Y.; writing—review and editing, W.Y., W.D., Y.L., C.L., T.W., K.W., C.C., N.Z., H.L. and C.D.; supervision, C.D.; project administration, W.Y. All authors have read and agreed to the published version of the manuscript.

Funding: This research is supported in part by the National Natural Science Foundation of China (Grant No. 62001374, 62105252, 62071376, 62005211, 62107033), the Sustainedly Supported Foundation by National Key Laboratory of Science and Technology on Space Microwave (Grant No. HTKJ2022KL504004), the Outstanding Youth Foundation of Xi'an branch, the Fifth Academy, Aerospace Science and Technology Group (Grant No. Y21-RCFYJQ1-05), State Key Laboratory of Applied Optics on Changchun Institute of Optics (Grant No. SKLAO2022001A12), and Guangdong Basic and Applied Basic Research Foundation (Grant No. 2020A1515111012).

Institutional Review Board Statement: Not applicable.

Informed Consent Statement: Not applicable.

Data Availability Statement: Data available on request.

Conflicts of Interest: The authors declare no conflict of interest.

References

1. Lawrie, B.; Pooser, R.; Maksymovych, P. Squeezing Noise in Microscopy with Quantum Light. *Trends Chem.* **2020**, *2*, 683–686. [CrossRef]
2. Lu, L.F.; Zhang, F. A deep tissue optical sensing. *Nat. Nanotechnol.* **2020**, *17*, 566–568. [CrossRef] [PubMed]
3. Degen, C.L.; Reinhard, F.; Cappellaro, P. Quantum sensing. *Rev. Mod. Phys.* **2017**, *89*, 035002. [CrossRef]
4. Kimble, H.J. The quantum internet. *Nature* **2008**, *453*, 1023–1030. [CrossRef]

5. Wang, Q.W.; Wang, Y.J.; Sun, X.C.; Tian, Y.H.; Li, W.; Tian, L.; Yu, X.D.; Zhang, J.; Zheng, Y.H. Controllable continuous variable quantum state distributor. *Opt. Lett.* **2021**, *46*, 1844–1847. [CrossRef]
6. Shi, S.P.; Tian, L.; Wang, Y.J.; Zheng, Y.H.; Xie, C.D.; Peng, K.C. Demonstration of channel multiplexing quantum communication exploiting entangled sideband modes. *Phys. Rev. Lett.* **2020**, *125*, 070502. [CrossRef]
7. Sun, X.C.; Wang, Y.J.; Tian, Y.H.; Wang, Q.W.; Tian, L.; Zheng, Y.H.; Peng, K.C. Deterministic and universal quantum squeezing gate with a teleportation like protocol. *Laser Photonics Rev.* **2021**, *16*, 2100329. [CrossRef]
8. Barz, S.; Fitzsimons, J.F.; Kashefi, E.; Walther, P. Experimental verification of quantum computation. *Nat. Phys.* **2013**, *9*, 727–731. [CrossRef]
9. Chua, S.S.Y.; Slagmolen, B.J.J.; Shaddock, D.A.; McClelland, D.E. Quantum squeezed light in gravitational-wave detectors. *Class. Quantum Grav.* **2014**, *31*, 183001. [CrossRef]
10. The LIGO Scientific Collaboration. A gravitational wave observatory operating beyond the quantum shot-noise limit. *Nat. Phys.* **2011**, *7*, 962–965. [CrossRef]
11. Purdy, T. Bright squeezed light reduces back-action. *Nat. Photonics* **2020**, *14*, 1–2. [CrossRef]
12. Taylor, A.T.; Lai, E.P.C. Current State of Laser-Induced Fluorescence Spectroscopy for Designing Biochemical Sensors. *Chemosensors* **2021**, *9*, 275. [CrossRef]
13. Yin, X.K.; Dong, L.; Wu, H.P.; Gao, M.; Zhang, L.; Zhang, X.S.; Liu, L.X.; Shao, X.P.; Tittel, F.K. Compact QEPAS humidity sensor in SF6 buffer gas for high-voltage gas power systems. *Photoacoustics* **2022**, *25*, 100319. [CrossRef] [PubMed]
14. Yin, X.K.; Gao, M.; Miao, R.Q.; Zhang, L.; Zhang, X.S.; Liu, L.X.; Shao, X.P.; Tittel, F.K. Near-infrared laser photoacoustic gas sensor for simultaneous detection of CO and H2S. *Optics Express* **2021**, *29*, 34258–34268. [CrossRef] [PubMed]
15. Yin, X.K.; Wu, H.P.; Dong, L.; Li, B.; Ma, W.G.; Zhang, L.; Yin, W.B.; Xiao, L.T.; Jia, S.T.; Tittel, F.K. Ppb-level SO_2 photoacoustic sensors with a suppressed absorption−desorption effect by using a 7.41 μm external-cavity quantum cascade laser. *ACS Sens.* **2020**, *5*, 549–556. [CrossRef]
16. Brida, G.; Genovese, M.; Berchera, I.R. Experimental realization of sub-shot-noise quantum imaging. *Nat. Photon.* **2010**, *4*, 227–230. [CrossRef]
17. Lawrie, B.J.; Lett, P.D.; Marino, A.M.; Pooser, R.C. Quantum Sensing with Squeezed Light. *ACS Photonics* **2019**, *6*, 1307–1318. [CrossRef]
18. Slusher, R.E.; Hollberg, L.W.; Yurke, B.; Mertz, J.C.; Valley, J.F. Observation of squeezed states generated by four-wave mixing in an optical cavity, *Phys. Rev. Lett.* **1985**, *55*, 2409–2412. [CrossRef]
19. Shelby, R.M.; Levenson, M.D.; Perlmutter, S.H.; DeVoe, R.G.; Walls, D.F. Broad-band parametric deamplification of quantum noise in an optical fiber. *Phys. Rev. Lett.* **1986**, *57*, 691–694. [CrossRef]
20. Schneider, K.; Lang, M.; Mlynek, J.; Schiller, S. Generation of strongly squeezed continuous-wave light at 1064 nm. *Opt. Express* **1998**, *2*, 59–64. [CrossRef]
21. Brooks, D.W.C.; Botter, T.; Schreppler, S.; Purdy, T.P.; Brahms, N.; Stamper-Kurn, D.M. Non-classical light generated by quantum-noise-driven cavity optomechanics. *Nature* **2012**, *488*, 476–480. [CrossRef] [PubMed]
22. Purdy, T.P.; Yu, P.L.; Peterson, R.W.; Kampel, N.S.; Regal, C.A. Strong optomechanical squeezing of light, *Phys. Rev. X* **2013**, *3*, 031012.
23. Safavi-Naeini, A.H.; Gröblacher, S.; Hill, J.T.; Chan, J.; Aspelmeyer, M.; Painter, O. Squeezed light from a silicon micromechanical resonator. *Nature* **2013**, *500*, 185–189. [CrossRef]
24. Vahlbruch, H.; Mehmet, M.; Danzmann, K.; Schnabel, R. Detection of 15 dB squeezed states of light and their application for the absolute calibration of photoelectric quantum efficiency *Phys. Rev. Lett.* **2016**, *117*, 110801. [CrossRef] [PubMed]
25. Khalaidovski, A.; Vahlbruch, H.; Lastzka, N.; Graf, C.; Danzmann, K.; Grote, H.; Schnabel, R. Long-term stable squeezed vacuum state of light for gravitational wave detectors. *Class. Quantum. Grav.* **2012**, *29*, 075001. [CrossRef]
26. Wang, Y.J.; Yang, W.H.; Zheng, Y.H.; Peng, K.C. A compact Einstein-Podolsky-Rosen entangled light source. *Chin. Phys. B* **2015**, *24*, 070303. [CrossRef]
27. Lu, H.D.; Su, J.; Zheng, Y.H.; Peng, K.C. Physical conditions of single-longitudinal-mode operation for high-power all-solid-state lasers, *Opt. Lett.* **2014**, *39*, 1117–1120.
28. Black, E.D. An introduction to Pound–Drever–Hall laser frequency stabilization. *Am. J. Phys.* **2001**, *69*, 79–87. [CrossRef]
29. Jin, X.L.; Su, J.; Zheng, Y.H.; Chen, C.Y.; Wang, W.Z.; Peng, K.C. Balanced homodyne detection with high common mode rejection ratio based on parameter compensation of two arbitrary photodiodes. *Opt. Express* **2015**, *18*, 23859–23866. [CrossRef]
30. Li, Z.X.; Ma, W.G.; Yang, W.H.; Wang, Y.J.; Zheng, Y.H.; Peng, K.C. Reduction of zero baseline drift of the Pound–Drever–Hall error signal with a wedged electro-optical crystal for squeezed state generation. *Opt. Lett.* **2016**, *41*, 3331–3334. [CrossRef]
31. Chen, C.Y.; Shi, S.P.; Zheng, Y.H. Low-noise, transformer-coupled resonant photodetector for squeezed state generation. *Rev. Sci. Instrum.* **2017**, *88*, 103101. [CrossRef] [PubMed]